

# PROGRESS IN APPLIED NUMERICAL ANALYSIS FOR COMPUTATIONAL FLUID DYNAMICS

M.B. GILES

*Oxford University Computing Laboratory*

*Wolfson Building, Parks Road, Oxford OX1 3QD, UK*

## 1. Introduction

The last 20 years have seen phenomenal progress in the development and application of CFD algorithms, advancing from 1D to 3D calculations, from steady to unsteady flows, from potential flow modelling to the Reynolds-averaged Navier-Stokes equations, from single-block structured grids to unstructured and hybrid grids, and from pure CFD applications to a wide variety of multi-disciplinary applications.

Much of this progress has been built upon a relatively small base of numerical analysis theory. The numerical stability of constant coefficient finite difference equations on infinite structured grids is determined using Fourier analysis. This also gives a necessary, and usually sufficient, local condition for stability when the coefficients of the finite difference equation vary smoothly. For unstructured grids, the CFL theorem has been the mainstay, giving a condition for stability which is necessary, and usually within a constant factor of 2 – 5 of being sufficient.

Truncation error (or modified equation) analysis is the basis for determining the order of accuracy of algorithms on structured grids, but for finite volume methods on unstructured grids this theory is inadequate. Many finite element methods have their own distinct mathematical theory, but the accuracy that is achieved in actual computations is often much better than the error bounds predicted by theory. With such a large discrepancy, it is not obvious that the numerical analysis provides a good basis for designing improved discretisations.

Perhaps one of the best examples of the relative strengths and weaknesses of engineering computations and numerical analysis has been in grid adaptation. Numerical analysis theory exists for some very simple applications, such as the Laplace equation. However, most developments in adap-

tive 3D computations using the Euler and Navier-Stokes equations have been with *ad hoc* adaptation criteria based on a combination of a very good understanding of fluid dynamics, knowledge of the truncation errors in flux evaluations, and a considerable amount of numerical experimentation.

My conjecture is that in the next 10 years there will continue to be great progress in the development and application of CFD algorithms, much of it in multi-disciplinary and design applications. However, I think algorithmic developments in ‘core’ areas of CFD, for example improving the accuracy of a discretisation, or the effectiveness of grid adaptation, will depend increasingly on more detailed numerical analysis of the accuracy and stability of existing algorithms. In doing so, the numerical analysis will have to cope with the following aspects of engineering computations:

- systems of equations
- nonlinearity
- irregular and unstructured grids
- boundary conditions
- high Reynolds number viscous flow
- multidisciplinary applications

This paper cannot attempt to survey the range of old and new theory in numerical analysis which can be applied to address these issues. Instead, it presents a number of recent analyses performed by the author:

- accuracy of quasi-1D shock capturing (Gil96)
- stability of aerothermal coupling (Gil95b)
- accuracy of aeroelastic coupling (Gil95c)
- stability of N-S computations on unstructured grids (Gil95a)

Each is motivated by an engineering application and involves the selection of a relevant model problem. Together, they illustrate the application of a selection of the numerical analysis theory which is able to treat some of the difficulties listed above.

## 2. Accuracy of quasi-1D shock capturing

This analysis was motivated by the question of how best to adapt grids for 2D and 3D transonic flow computations in which there are shocks. Ideally, the criterion will lead to the adaptation of only those cells in which large flow gradients generate large numerical errors. Unfortunately, at present there is no complete theory of *a posteriori* error estimation for the discretisation of nonlinear p.d.e.'s, on which to base rigorous adaptation criteria and so they have instead been developed based on a combination of model linear p.d.e.'s, engineering intuition and practical experience (e.g. (LMZ86; MJ87; PVMZ87; Dan88; WHMM93)).

One typical adaptation parameter that is used is  $A_p = h|\delta p|$ , where  $h$  is some measure of the cell length, and  $\delta p$  is a first difference of the pressure field. At shocks,  $\delta p$  is independent of the cell size and so the shock cells are adapted repeatedly until  $h$  is sufficiently small that  $A_p$  falls below the adaptation threshold. Away from shocks,  $A_p \approx h^2|\nabla p|$ , and so the adapted grid resolution is related to the flow gradient, as desired.

In designing adaptation criteria such as this which will generate a large number of adapted cells at shocks and so obtain very thin discrete shocks, it is implicitly assumed that the shock would otherwise cause substantial numerical errors. The lift on a wing is one of the most important engineering quantities obtained from a solution of the Euler equations. For such a calculation it appears, intuitively, that since the shock is 'smeared' over one or two cells there must be an error in the lift prediction of order  $h_s \Delta p$  where  $h_s$  is the cell size at the shock and  $\Delta p$  is the jump in pressure across the shock. This appears to be the basis for the particular adaptation criterion above, but other adaptation criteria also lead to very substantial refinement of shock cells and so the belief in a significant first order error at shocks seems widespread although not stated.

### 2.1. ANALYSIS

The model problem which was selected is the discretisation of transonic inviscid flow in a quasi-1D diverging duct. The steady quasi-1D Euler equations in conservative form are

$$\frac{d}{dx}(AF) - \frac{dA}{dx}P = 0, \quad (1)$$

where  $U$  is the state vector and  $F$  and  $P$  are the usual flux vectors given by

$$U = \begin{pmatrix} \rho \\ \rho u \\ \rho E \end{pmatrix}, \quad F = \begin{pmatrix} \rho u \\ \rho u^2 + p \\ \rho u H \end{pmatrix}, \quad P = \begin{pmatrix} 0 \\ p \\ 0 \end{pmatrix}. \quad (2)$$

$A(x)$  is the cross-sectional area of the duct which, for convenience, is assumed to be locally constant at the two ends.

At the supersonic inflow at  $x=0$ , the entire state vector  $U(0)$  is specified. At the subsonic outflow at  $x=1$ , the static pressure is specified. Integration of Equation (1) over the domain gives

$$[AF]_0^1 = \int_0^1 \frac{dA}{dx} P dx = \begin{pmatrix} 0 \\ D \\ 0 \end{pmatrix}, \quad (3)$$

where the ‘drag’  $D$  (the force exerted by the sidewall on the fluid) is defined as

$$D = \int_0^1 p \frac{dA}{dx} dx. \quad (4)$$

The first and third components of Equation (3) together with the one outflow boundary condition totally specify the three components of  $U(1)$  given that  $U(0)$  has already been specified. The second component of Equation (3) then defines  $D$  uniquely as a function of the boundary conditions independent of the precise variation of  $p(x)$  or  $A(x)$  between the end points. This is the key in determining the accuracy with which the discretisation approximates the quantity

$$\int_0^1 p dx$$

which represents the lift in 2D and 3D Euler calculations for lifting bodies.

The full details of the numerical analysis are presented in Reference (Gil96), but the outline approach is as follows. The analysis considers steady discrete equations of the following conservative form

$$A_{j+1/2} F_{j+1/2} - A_{j-1/2} F_{j-1/2} - (A_{j+1/2} - A_{j-1/2}) P_j = 0, \quad (5)$$

on a computational grid with uniform mesh spacing  $h$ .

The three components of the discrete solution at the inflow are specified as boundary conditions. Because the discretisation is conservative, mass and energy conservation together with the specification of the static pressure at the outflow fully determine the three components of the discrete solution at the outflow as well. Momentum conservation then implies that  $D_h$ , the discrete equivalent of the ‘drag’, is obtained exactly.

The drag integral can be split into two pieces, a ‘shock’ piece from a region of width  $O(h)$  spanning the shock, and a ‘smooth’ piece from the regions on either side of the shock in which the flow is smooth.

In the smooth flow regions, the solution error is  $O(h^m)$  where  $m$  is the order of the truncation error. The corresponding errors in the ‘smooth’

pieces of the discrete drag and lift are also  $O(h^m)$ . Since the combined drag integral is exact, the error in the shock piece of the discrete drag must be equal and opposite, and so is  $O(h^m)$ . Reference (Gil96) presents an asymptotic analysis which shows that, as a consequence, the error in the ‘shock’ piece of the discrete lift integral is  $O(h^2)$ . Provided  $m \geq 2$ , this means that the total error in the discrete lift integral is also  $O(h^2)$ .

Writing the total lift error as

$$L_h - L = C_h h^2, \quad (6)$$

there is nothing in the analysis to suggest that  $C_h$  should asymptote to a constant as  $h \rightarrow 0$ . The proven second order accuracy only requires that  $C_h$  be bounded, leaving the possibility that  $C_h$  may depend on the location of the shock within the shock cell (e.g. whether the shock is at a grid node or halfway between two nodes).

## 2.2. NUMERICAL RESULTS

Numerical results were obtained using a discretisation in which the numerical smoothing is a blend of second and fourth difference terms. The duct geometry and boundary conditions were chosen so that the peak Mach number on the upstream side of the shock was 1.3. The steady-state discrete solutions were obtained by a fully-converged Runge-Kutta time-marching procedure. Figure 1 shows the Mach number distribution for the solution near the shock using a uniform grid of 64 points.

To investigate the effect of mesh resolution, a sequence of grids was used, with the number of grid points ranging from 64 to 192. For each grid, the influence of the shock position relative to the grid nodes was investigated by performing a number of calculations with the grid displaced by an amount  $\delta x$  in the range  $0 \leq \delta x \leq h$ . Figure 2a) shows the errors in the computed lift. The ‘error bar’ indicates the range of values obtained depending on the position of the shock relative to the grid. Figure 2b) plots the magnitude of these error bars  $L_h^{max} - L_h^{min}$ . Note that in both figures the quantities are plotted against  $h^2$ , not  $h$ . The linear behaviour in Figure 2b) corresponds to the second order ‘shock’ component of the error, as predicted by the numerical analysis, with  $C_h$  being a function of the shock position. Figure 2a) also shows an almost linear behaviour for small values of  $h$ , but for larger values the error increases more rapidly, due to the ‘smooth’ component of the error which is  $O(h^3)$ . Figure 2a) also illustrates the possibility for non-monotonic convergence as  $h$  is refined; for sufficiently small values of  $h$  there are some points within the error bar which show an overprediction of the lift, while others show an underprediction.

The result that the lift is determined with second order accuracy for the model quasi-1D problem is surprising and counter-intuitive. If one performs

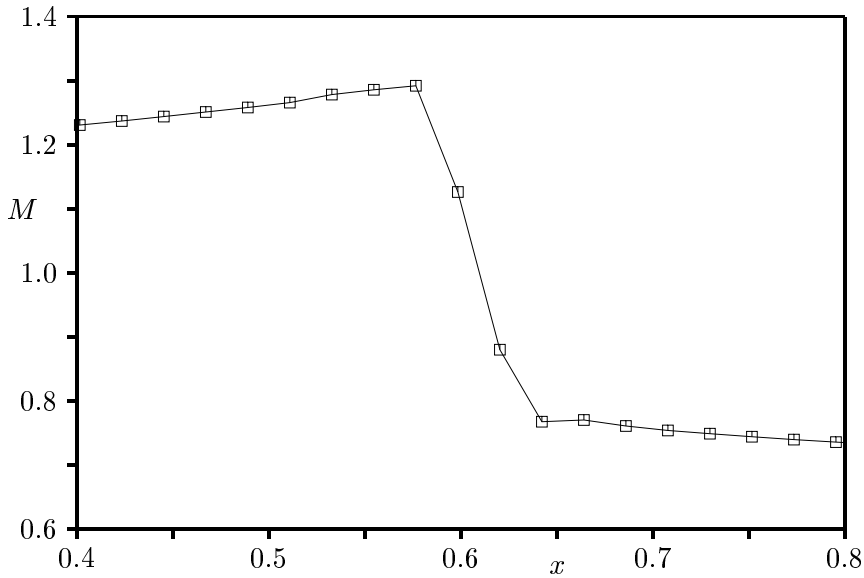


Figure 1. Mach number distribution near the shock

numerical integration of the analytic solution at the discrete grid points using the trapezoidal method, the integration error is  $O(h)$  since the value of the trapezoidal integral will be independent of the precise location of the shock within the shock cell. A similar argument applies to the use of any other numerical integration scheme. Since the asymptotic analysis and numerical evidence show that the discrete lift is  $O(h^2)$ , there must be an equal but opposite error which is also  $O(h)$ . This can only be due to a  $O(1)$  difference between the analytic solution and the discrete solution at the grid points near the shock.

### 2.3. RELEVANCE TO 2D/3D APPLICATIONS

There is obviously a question about the relevance of the quasi-1D model problem to the 2D and 3D computations which are of real engineering interest. Unpublished grid refinement studies by Jameson show a variety of behaviour for different test cases. Almost all show convergence in lift and drag to be faster than first order. A substantial fraction, but not the majority, show clear second order convergence with the error proportional to  $h^2$ . The majority show very rapid convergence which does not appear to be proportional to  $h^m$  for any value of  $m$ ; in many cases the convergence is not even monotonic. These results are consistent with the quasi-1D analysis. However, extending the rigorous numerical analysis from the quasi-1D duct problem to a 2D airfoil problem may prove to be very difficult.

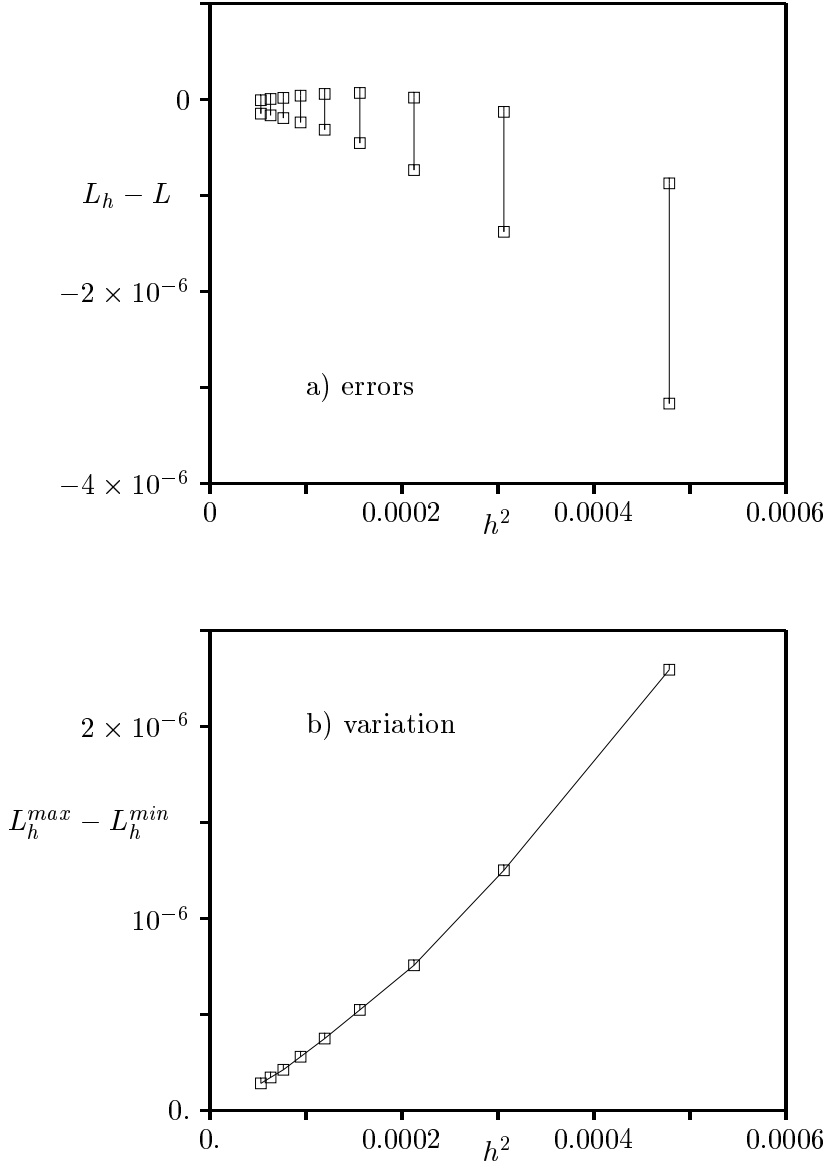


Figure 2. Errors and variation in computed lift

### 3. Stability of aerothermal analysis

This research was motivated by interest in numerical procedures for combined aerothermal analysis, coupling a thermal diffusion analysis of the heat flux in a solid turbine blade with a Navier-Stokes computation of the surrounding fluid.

One approach to the numerical approximation of this situation would be the use of a single consistent fully-coupled discretisation modelling both the solid and the fluid, plus the boundary conditions at the interfaces (MMHC89).

However, in practice, a simpler approach is to link two separate codes modelling the solid and fluid, exchanging information at the interface between the two (AWP94; CTB94; HV95; BLpB95). Both CFD codes and thermal analysis codes usually have the capability to specify either the temperature or the heat flux at boundaries. A natural choice therefore for coupling these codes is to specify the surface temperature at the interface in one code, taking the value from the other code, and specify the boundary heat flux in the second code, taking its value from the first code (AWP94; CTB94). A concern was whether there is any possibility that the coupling procedure could introduce a spurious numerical instability. Therefore, the numerical stability of a model 1D problem was analysed.

#### 3.1. MODEL PROBLEM

As indicated in Figure 3, the 1D model problem has a solid in the region  $x < 0$ , and a fluid in  $x > 0$ . In the solid, the evolution of the unsteady temperature is governed by the diffusion equation

$$c_- \frac{\partial T}{\partial t} = -\frac{\partial q}{\partial x}, \quad q = -k_- \frac{\partial T}{\partial x}, \quad (7)$$

in which  $T(x, t)$  is the temperature,  $q(x, t)$  is the heat flux, and  $c_-$  and  $k_-$  are the heat capacity and conductivity, respectively, which are taken to be uniform.

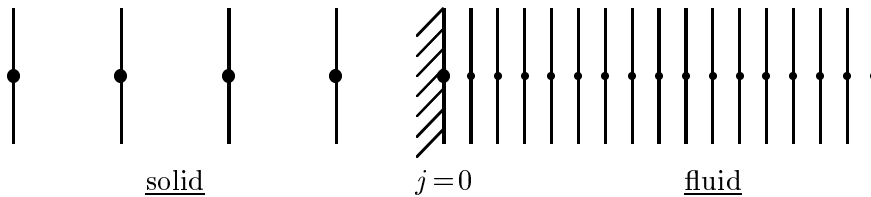


Figure 3. 1D geometry for aerothermal analysis

In the fluid, the convection velocity is neglected, and so the Navier-Stokes equations reduce to a thermal diffusion equation of the same form, but with uniform heat capacity  $c_+$  and conductivity  $k_+$ .

At  $x=0$ , the interface conditions are that  $T$  and  $q$  must be continuous. The boundary conditions as  $x \rightarrow \pm\infty$  are that  $q \rightarrow 0$ .

### 3.2. STABILITY ANALYSIS

Using a computational grid with uniform spacing  $\Delta x_+$  for the fluid, and uniform spacing  $\Delta x_-$  for the solid, explicit Forward Euler central space differencing of the diffusion equation gives the algorithm

$$\frac{c_{\pm}\Delta x_{\pm}}{\Delta t}(T_j^{(n+1)} - T_j^{(n)}) = \frac{k_{\pm}}{\Delta x_{\pm}}(T_{j+1}^{(n)} - 2T_j^{(n)} + T_{j-1}^{(n)}), \quad (8)$$

on either side of the interface, i.e. for  $j \neq 0$ .

This can be re-expressed as

$$(T_j^{(n+1)} - T_j^{(n)}) = d_{\pm}(T_{j+1}^{(n)} - 2T_j^{(n)} + T_{j-1}^{(n)}), \quad j \neq 0, \quad (9)$$

where

$$d_{\pm} \equiv \frac{k_{\pm}\Delta t}{c_{\pm}\Delta x_{\pm}^2}. \quad (10)$$

Standard Fourier analysis shows that this is stable provided  $d_{\pm} < \frac{1}{2}$ .

At the interface, we choose to enforce continuity of temperature and heat flux by using the solid surface temperature as the boundary condition for the fluid, and using the fluid surface heat flux as the boundary condition for the solid. To be precise, the calculation of  $T_1^{(n+1)}$  in the fluid uses the temperature  $T_0^{(n)}$  from the solid, and the temperature  $T_0^{(n+1)}$  in the solid is calculated from

$$\frac{c_- \Delta x_-}{2\Delta t}(T_0^{(n+1)} - T_0^{(n)}) = -q_w - \frac{k_-}{\Delta x_-}(T_0^{(n)} - T_{-1}^{(n)}), \quad (11)$$

with the fluid surface heat flux being evaluated by a first order one-sided difference (HV95),

$$q_w = -\frac{k_+}{\Delta x_+}(T_1^{(n)} - T_0^{(n)}). \quad (12)$$

It is more convenient to consolidate these last two equations into the following equation,

$$T_0^{(n+1)} = T_0^{(n)} - 2d_- (T_0^{(n)} - T_{-1}^{(n)}) + 2rd_+ (T_1^{(n)} - T_0^{(n)}), \quad (13)$$

in which  $r$  is the ratio of the thermal capacities of the computational cells on either side of the interface,

$$r = \frac{c_+ \Delta x_+}{c_- \Delta x_-}. \quad (14)$$

The interface stability analysis uses the well-established theory of Godunov and Ryabenkii (GR64; RM67), in which the task is to investigate the existence of separable normal modes of the form

$$T_j^{(n)} = z^n f_j. \quad (15)$$

The discretisation is unstable if the difference equation admits such solutions which satisfy the far-field boundary conditions,  $f_j \rightarrow 0$  as  $j \rightarrow \pm\infty$ , and have  $|z| > 1$ , giving exponential growth in time. The form of the solution is very similar to that of Fourier modes, except that the amplitude of the spatial oscillation decays exponentially away from the interface.

For this application the normal mode must be of the form

$$T_j^{(n)} = \begin{cases} z^n \kappa_-^j, & j \leq 0 \\ z^n \kappa_+^j, & j \geq 0 \end{cases}. \quad (16)$$

The difference equations, Equation (9) and Equation (13), are satisfied provided the three variables  $z, \kappa_-, \kappa_+$  satisfy the following equations.

$$\begin{aligned} z &= 1 + d_-(\kappa_- - 2 + \kappa_-^{-1}) \\ z &= 1 + 2d_-(\kappa_-^{-1} - 1) + 2rd_+(\kappa_+ - 1) \\ z &= 1 + d_+(\kappa_+ - 2 + \kappa_+^{-1}) \end{aligned} \quad (17)$$

Solving the first of these equations to obtain  $\kappa_-^{-1}$  gives

$$\kappa_-^{-1} = 1 - \frac{1-z}{2d_-} \left( 1 \pm \sqrt{1 - \frac{4d_-}{1-z}} \right). \quad (18)$$

To satisfy the far-field boundary conditions as  $j \rightarrow -\infty$  it is necessary to choose the negative square root when the argument is real and positive; when it is complex, the choice of root is defined by the requirement that  $|\kappa_-^{-1}| < 1$ . Solving the third of the equations similarly to obtain  $\kappa_+$ , and substituting these into the second equation gives the following nonlinear equation for  $z$ .

$$\sqrt{1 - \frac{4d_-}{1-z}} - r \left( 1 - \sqrt{1 - \frac{4d_+}{1-z}} \right) = 0 \quad (19)$$

There is no simple closed form solution to this, giving  $z$  as an explicit function of the parameters  $d_-$ ,  $d_+$ ,  $r$ , but analysis of this equation reveals that  $|z| < 1$  if, and only if,

$$r < \frac{\sqrt{1 - 2d_-}}{1 - \sqrt{1 - 2d_+}}. \quad (20)$$

The full details are presented in (Gil95b).

This analysis is supported by the numerical results presented in Figure 4. The computations use the finite domain  $-2000 \leq j \leq 2000$ , initial conditions  $T_j^0 = -1$  for  $j < 0$  and  $T_j^0 = 1$  for  $j \geq 0$  and boundary conditions  $T_{-2000}^{(n)} = -1$ ,  $T_{2000}^{(n)} = 1$ .  $d_-$  and  $d_+$  are both taken to be  $\frac{3}{8}$ , for which the analysis above predicts the coupled system to be stable only for  $r < 1$ .

Figure 4 shows two sets of results with  $T_j^{(n)}$  plotted every 25 iterations. In a),  $r = 0.99$  and the solution appears to be stable, with a slowly decaying interface transient, while in b),  $r = 1.01$  and the solution is clearly unstable.

Reference (Gil95b) also analyses the stability of two other algorithms. One is a hybrid algorithm in which the fluid is discretised using the same explicit algorithm, but the solid is discretised using an implicit algorithm. The other uses an implicit discretisation for both the solid and the fluid, but an explicit updating of the boundary conditions for each. For both of these algorithms, the analysis reveals that the stability depends on the parameters  $r$ ,  $d_-$  and  $d_+$ , with the coupling being unstable when  $r \gg 1$  and stable when  $r \ll 1$ .

In practice, typical values for  $c_{\pm}$  and  $\Delta x$  usually result in  $r \ll 1$ , and so the coupled fluid/structural calculations will be stable. This is based on the assumption that the fluid takes its surface temperature from the solid, and the solid takes its surface heat flux from the fluid. If the roles are reversed, specifying the heat flux into the fluid and the surface temperature of the solid, then the above analysis remains valid with the fluid in  $x < 0$  and the solid in  $x > 0$ . In this case,  $r \gg 1$ , and so the coupling would be unstable.

### 3.3. CONCLUSIONS

The stability analysis shows the viability of a loosely-coupled approach to computing the temperature and heat flux in coupled fluid/structure interactions. The key point to achieving numerical stability is the use of Dirichlet boundary conditions for the fluid calculation and Neumann boundary conditions for the structural calculation. Although the analysis is performed for a 1D model diffusion equation, this conclusion should remain valid for the real engineering calculations in which the 3D diffusion equation is used to model the heat flux in the structure and the 3D Navier-Stokes equations are used to model the behaviour of the fluid.

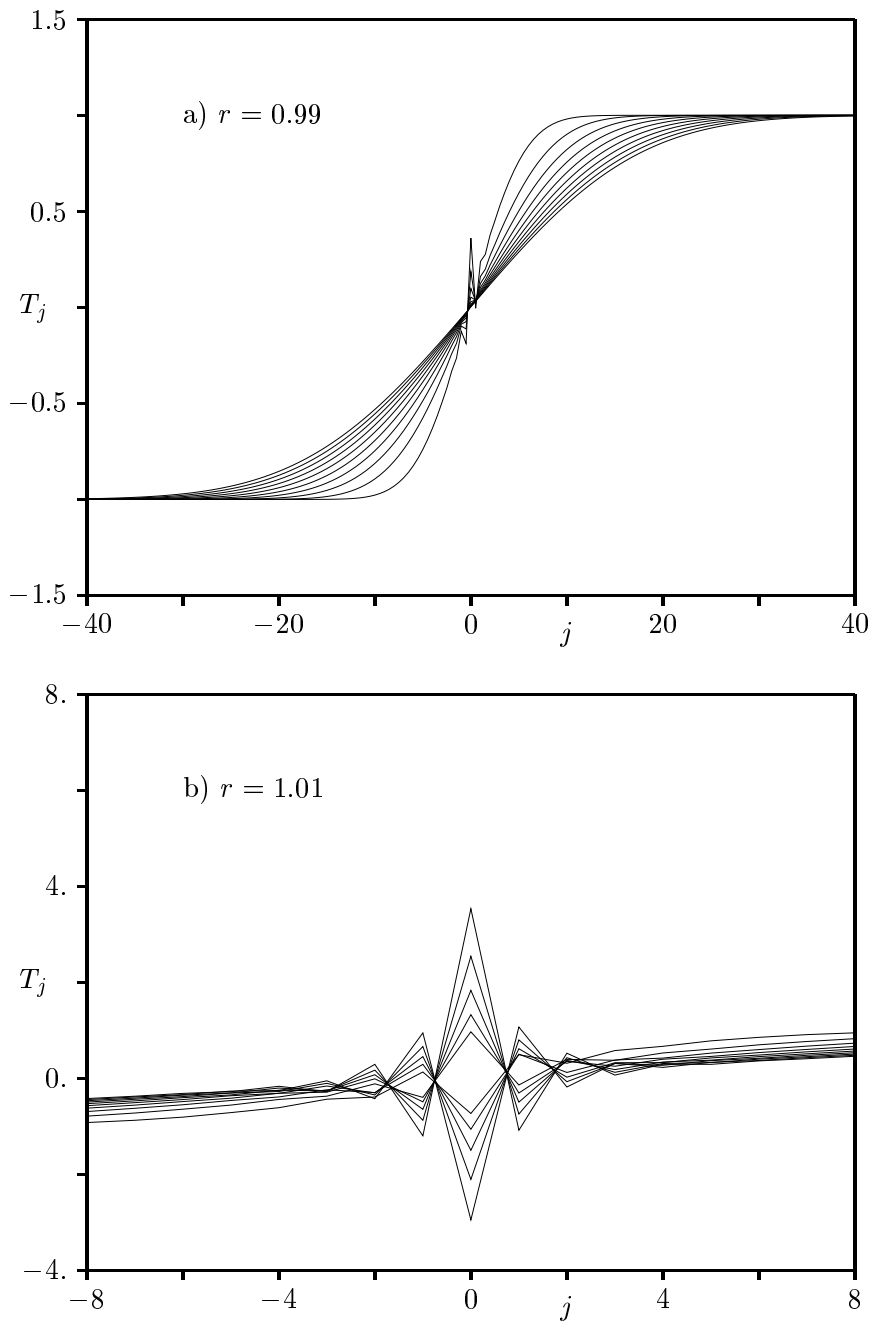


Figure 4. Aerothermal coupling with results every 25 iterations

#### 4. Accuracy of aeroelastic coupling

The possible flutter of aircraft wings and turbomachinery blades can now be investigated by the simultaneous solution of the coupled 3D nonlinear p.d.e.'s describing the unsteady aerodynamics and structural dynamics of the application (Gur90a; Gur90b; MI95; NH92). However, such calculations are computationally demanding, preventing extensive investigations of some of the underlying algorithmic issues. One issue is whether the coupling procedure may introduce a spurious Godunov–Ryabenkii numerical instability, unrelated to the real flutter instabilities which are the focus of engineering attention. Another is the accuracy of the resulting coupled analysis, particularly when there are very few timesteps per period of oscillation.

To investigate these issues, a model 1D problem was constructed, and a number of different discretisations were analysed and tested numerically (Gil95c).

##### 4.1. MODEL PROBLEM

As illustrated in Figure 5, the 1D model problem consists of a wall oscillating about  $x=0$ , and a semi-infinite fluid in  $x>0$ .

Neglecting all viscous effects, the fluid dynamics is modelled by the inviscid acoustic equations expressed as a coupled system of first order differential equations for the pressure,  $p$ , and velocity,  $u$ ,

$$\frac{\partial}{\partial t} \begin{pmatrix} p \\ u \end{pmatrix} + \begin{pmatrix} 0 & \rho c^2 \\ \frac{1}{\rho} & 0 \end{pmatrix} \frac{\partial}{\partial x} \begin{pmatrix} p \\ u \end{pmatrix} = 0. \quad (21)$$

Here  $\rho$  and  $c$  are the density and speed of sound, respectively, of the undisturbed fluid.

The dynamics of the wall's motion are modelled by a simple mass-spring system subject to the external unsteady aerodynamic pressure.

$$m \ddot{x}_w + m\omega_0^2 x_w = -p(0, t). \quad (22)$$

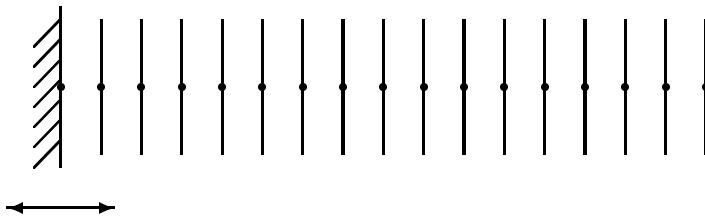


Figure 5. 1D geometry for aeroelastic analysis

Here  $m$  represents the mass per unit area and  $\omega_o$  is the natural frequency of oscillation in the absence of any aerodynamic coupling.

There is also a kinematic compatibility condition, requiring that the velocity of the wall must match that of the fluid.

$$\dot{x}_w(t) = u(0, t). \quad (23)$$

In the far-field, the boundary condition is the radiation condition, that all waves should be outgoing, travelling away from the oscillating wall.

This simple model problem admits an eigenmode solution of the form

$$\begin{aligned} x_w(t) &= X e^{i\omega t}, \\ p(x, t) &= P e^{i\omega(t-x/c)}, \\ u(x, t) &= U e^{i\omega(t-x/c)}, \end{aligned} \quad (24)$$

where

$$\frac{\omega}{\omega_o} = \sqrt{1 - d^2} + id \approx 1 + id - \frac{1}{2}d^2, \quad (25)$$

and

$$d = \frac{\rho c}{2m\omega_o}. \quad (26)$$

The positive imaginary component of  $\omega$  indicates the amplitude of the wall's oscillation is decaying exponentially; this is because the wall's kinetic and potential energy is being converted into radiating acoustic energy of the fluid.

$d$  is the non-dimensional damping factor which plays a critical role in the aeroelastic analysis. In engineering applications, it is usually in the range 0.005 – 0.02 for turbomachinery flutter, and in the range 0.05 – 0.2 for aircraft wing flutter.

#### 4.2. NUMERICAL ANALYSIS

Using first order upwinding for the CFD, with either explicit or implicit time differencing, the discrete equivalent of the far-field radiation condition leads to the conclusion that the discrete characteristic variables corresponding to the incoming acoustic mode are all zero. As a consequence, the pressure and velocity at the wall node,  $j=0$ , are related by

$$p_0^{(n)} = \rho c u_0^{(n)}. \quad (27)$$

A central difference approximation to the wall dynamics gives

$$\frac{m}{\Delta t^2} \left( x_w^{(n+1)} - 2x_w^{(n)} + x_w^{(n-1)} \right) + m\omega_o^2 x_w^{(n)} = -p_0^{(n)}. \quad (28)$$

The final discrete equation is the kinematic compatibility condition. A simple first order approximation of this is

$$\frac{1}{\Delta t} \left( x_w^{(n+1)} - x_w^{(n)} \right) = u_0^{(n)}. \quad (29)$$

An eigenmode of the form

$$\begin{aligned} x_w^{(n)} &= X z^n, \\ p_0^{(n)} &= P z^n, \\ u_0^{(n)} &= U z^n, \end{aligned} \quad (30)$$

is a solution if, and only if,  $z$  satisfies the equation

$$z - 2 + z^{-1} + (\omega_0 \Delta t)^2 = -2d \omega_0 \Delta t (1 - z^{-1}). \quad (31)$$

It can be shown that, for  $0 < d < 1$ , the roots of this quadratic equation have magnitude less than unity provided

$$\omega_0 \Delta t \leq \sqrt{4 + d^2} - d < 2. \quad (32)$$

Thus, there is no numerical instability provided there are more than 3 timesteps per period of natural oscillation of the wall.

To determine the accuracy of the discretisation, we let  $z = e^{i\omega \Delta t}$  and performing a Taylor series expansion in both  $d$  and  $\omega_0 \Delta t$  to obtain

$$\frac{\omega}{\omega_0} \approx 1 + id - \frac{1}{2}d^2 + \frac{1}{2}d\omega_0 \Delta t + id^2 \omega_0 \Delta t + \frac{1}{24}(\omega_0 \Delta t)^2 + O(d^4, (\omega_0 \Delta t)^4). \quad (33)$$

This shows that the first order error in the coupling produces a first order error in both the real and imaginary components of the complex frequency, corresponding to the frequency and damping rate of the coupled oscillation.

The accuracy of this analysis is shown in Figure 6. Numerical calculations were performed for  $\omega_o \Delta t = 0.02, 0.05, 0.1, 0.2$  (corresponding approximately to 300, 120, 60, 30 timesteps per period) and values of  $d$  in the range 0.005 – 0.1. Each calculation was performed for 10,000 iterations, and from the results the frequency and damping rate were deduced. These are presented as solid lines in the two parts of Figure 6, while the dashed lines show the predictions from the asymptotic analysis above. The agreement is excellent over the whole parameter range studied.

For a typical flutter frequency and a timestep limited by the explicit CFL stability restriction  $\frac{c\Delta t}{\Delta x} < 1$  for a typical grid resolution,  $\omega_0 \Delta t$  will be in the range  $10^{-3} - 10^{-2}$ . In this case, the errors in both the frequency and the damping are negligible compared to other errors such as modelling approximations and uncertainty about structural damping factors. However,

when using implicit methods (Jam91; RBY93), the timestep is no longer limited by the CFL condition and  $\omega_0 \Delta t$  will typically be  $O(10^{-1})$ . In this case the first order coupling is no longer sufficiently accurate.

Reference (Gil95c) contains analyses of three alternative discretisations of the compatibility equation, all of which are second order. The best of the three is the implicit discretisation

$$\frac{1}{2\Delta t} \left( x_w^{(n+1)} - x_w^{(n-1)} \right) = u_0^{(n)}, \quad (34)$$

which can be implemented using a predictor/corrector procedure. Some alternative discretisations of the wall dynamic equations are also analysed and tested numerically. This includes the very accurate state-transition algorithm used by Rausch *et al* (RBY93).

#### 4.3. CONCLUSIONS

One conclusion from all of the analyses and comparisons with numerical experiments is that the asymptotic numerical analysis is very accurate in predicting the accuracy of the coupled aeroelastic damping and frequency when there are at least 30 timesteps per period and the non-dimensional damping parameter  $d$  is in the range  $0.005 - 0.1$ .

If an explicit CFD algorithm is used for the aerodynamic equations, then for typical flutter frequencies and aerodynamic grid resolution the number of timesteps per period will so large that any algorithm for the discretisation of the structural dynamics and the kinematic boundary condition will be sufficiently accurate provided it is at least second order accurate for the uncoupled vibration.

If, on the other hand, an implicit CFD algorithm is used for the aerodynamic equations, then it is possible that there may be as few as 30 timesteps per period. In this case it is necessary to use a discretisation which is second-order accurate for both the uncoupled and coupled systems. For turbomachinery applications with extremely low levels of structural and aerodynamic damping, it is also best to avoid the use of the many standard structural dynamics algorithms which cause spurious numerical damping of the uncoupled wall dynamics.

Although the real 3D aeroelastic applications (which can exhibit unstable flutter) are quite different to this model problem (which is always stable) it is thought these conclusions remain valid for the engineering applications of interest. Further discussion of this point is presented in Reference (Gil95c).

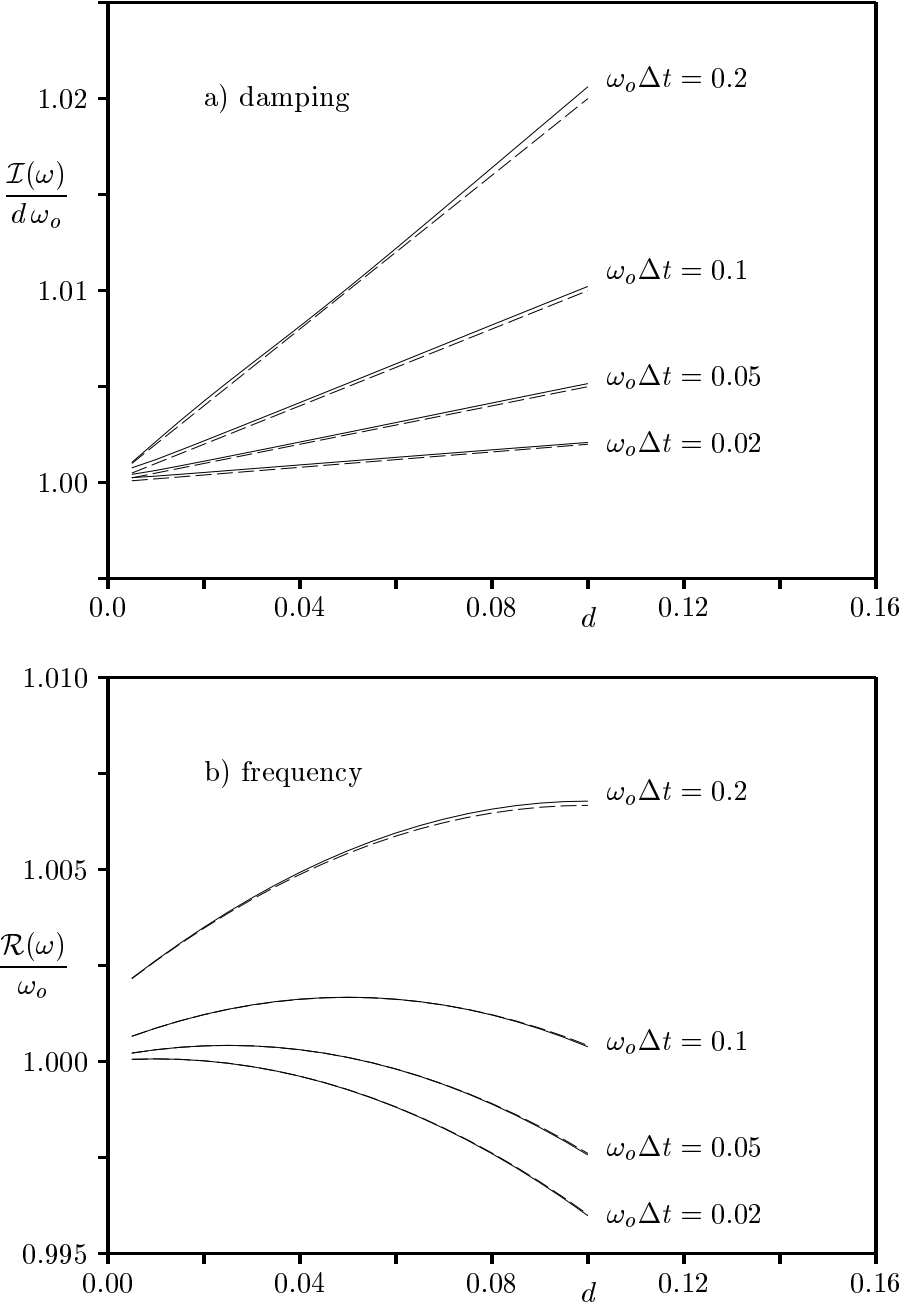


Figure 6. Aeroelastic damping and frequency using first order coupling algorithm (solid lines – numerical computation; dashed lines – numerical analysis)

## 5. Stability of N-S discretisation

### 5.1. INTRODUCTION

Inviscid flow calculations are now being performed almost routinely on unstructured grids for complete aircraft geometries (WHMM93; PPM93; RBY93; CG95). Many researchers are now working on the development of more accurate and more efficient Navier-Stokes discretisations, and these calculations will also become routine in the next five years.

This raises the problem of determining the timestep stability limit for explicit time-marching methods. Because the grid is unstructured, standard Fourier analysis is not applicable. The CFL theorem still applies, giving an upper bound for the maximum stable timestep and an rough estimate of the actual stability limit. However, it could be that these timestep stability limits are unnecessarily restrictive leading to a large increase in computational cost. This is likely to be particularly true for 3D computations, for which it is much harder to avoid poorly shaped computational cells.

The analysis discussed here, (Gil95a), uses recent theoretical developments in numerical analysis. A Galerkin spatial discretisation of the Navier-Stokes equations leads to a coupled system of semi-discrete equations which is solved using Runge-Kutta time-marching. The stability of this is analysed using the concept of *algebraic stability* developed by Spijker and others. In the case of the Euler equations, this leads to stability conditions which are equivalent to those obtained by Giles using an energy analysis method (RM67; Gil87).

### 5.2. NAVIER-STOKES DISCRETISATION

The equations which are considered are a linearised form of the Navier-Stokes equations, for perturbations from a steady-state which is uniform apart from possible variations in the viscosity and conductivity. A periodic domain is considered to avoid the complications of boundary conditions. Changing from the usual conservation variables to symmetrising variables  $U$  (GS78; AG81), it can be shown that the ‘energy’  $\iiint \|U\|^2 dV$  is non-increasing, and so the flow is stable.

Using a Galerkin spatial discretisation of the p.d.e. leads to a semi-discrete system of equations of the form

$$M \frac{dU}{dt} = (C+D)U. \quad (35)$$

The ‘mass’ matrix  $M$  and the diffusion matrix  $D$  are both symmetric, and positive definite and positive semi-definite, respectively. Furthermore, the

convection matrix  $C$  is anti-symmetric. As a consequence of these properties, the semi-discrete 'energy'  $U^T M U$  is non-increasing and so the semi-discrete solution is also stable.

### 5.3. STABILITY THEORY FOR RUNGE-KUTTA METHODS

Discretisation of the scalar o.d.e.

$$\frac{du}{dt} = \lambda u, \quad (36)$$

using an explicit Runge-Kutta method with timestep  $k$  yields a difference equation of the form

$$u^{(n+1)} = L(\lambda k) u^{(n)} \quad (37)$$

where  $L(z)$  is a polynomial function of degree  $p$

$$L(z) = \sum_{m=0}^p a_m z^m, \quad (38)$$

with  $a_0 = a_1 = 1$ ,  $a_p \neq 0$ . Discrete solutions of this difference equation on a finite time interval  $0 \leq t \leq t_0$  will converge to the analytic solution as  $k \rightarrow 0$ . In addition, the discretisation is said to be *absolutely stable* for a particular value of  $k$  if it does not allow exponentially growing solutions as  $t \rightarrow \infty$ ; this is satisfied provided  $\lambda k$  lies within the stability region  $S$  in the complex plane defined by

$$S = \{z : |L(z)| \leq 1\}. \quad (39)$$

Suppose now that a real square matrix  $A$  has a complete set of eigenvectors and can thus be diagonalised,

$$A = T \Lambda T^{-1}, \quad (40)$$

with  $\Lambda$  being the diagonal matrix of eigenvalues of  $A$ . The Runge-Kutta discretisation of the coupled system of o.d.e.'s,

$$\frac{dU}{dt} = AU, \quad (41)$$

can be written as

$$U^{(n+1)} = L(kA) U^{(n)} = T L(k\Lambda) T^{-1} U^{(n)}, \quad (42)$$

and hence

$$U^{(n)} = T (L(k\Lambda))^n T^{-1} U^{(0)}. \quad (43)$$

The necessary and sufficient condition for absolute stability as  $n \rightarrow \infty$ , requiring that there are no discrete solutions which grow exponentially

with  $n$ , is therefore that  $|L(k\lambda)| \leq 1$ , or equivalently  $k\lambda$  lies in  $S$ , for all eigenvalues  $\lambda$  of  $A$ . If this condition is satisfied, then using  $L_2$  vector and matrix norms it follows that

$$\|U^{(n)}\| \leq \|T\| \|L(k\Lambda)\|^n \|T^{-1}\| \|U^{(0)}\| \leq \kappa(T) \|U^{(0)}\|, \quad (44)$$

where  $\kappa(T)$  is the condition number of the eigenvector matrix  $T$ .

If the matrix  $A$  is normal, meaning that it has an orthogonal set of eigenvectors then the eigenvectors can be normalised so that  $\kappa(T) = 1$ . In this case,  $\|U^{(n)}\|$  is a non-increasing function of  $n$  and  $\|U^{(n)}\|^2$  represents a non-increasing ‘energy’ which could be used in an energy stability analysis. If  $A$  is not normal, then the growth in  $\|U^{(n)}\|$  is bounded by the condition number of the eigenvector matrix,  $\kappa(T)$ . Unfortunately, this can be very large indeed, allowing a very large transient growth in the solution even when for each eigenvalue  $k\lambda$  lies strictly inside the stability region  $S$  and so  $\|U^{(n)}\|$  must eventually decay exponentially. This problem can be particularly acute when the matrix  $A$  comes from the spatial discretisation of a p.d.e. in which case there is then a family of discretisations arising from a sequence of computational grids of decreasing mesh spacing  $h$ . It is possible in such circumstances for the sequence of condition numbers  $\kappa(T)$  to grow exponentially, with an exponent inversely proportional to the mesh spacing (RT92).

The stability of discretisations of systems of o.d.e.’s with non-normal matrices has been a major research topic in the numerical analysis community in recent years (RT92; KW93; KLS87; LS91; RT90; Red91; LN91; vDK93). Ideally, one would hope to prove *strong stability*,

$$\|U^{(n)}\| \leq \gamma \|U^{(0)}\|, \quad (45)$$

with  $\gamma$  being a constant which is not only independent of  $n$  but is also a uniform bound applying to all matrices in the family of spatial discretisations for different mesh spacings  $h$  but with the timestep  $k$  being a function of  $h$ . However, at present, the conditions under which strong stability can be proved are too restrictive to be useful in practical computations. Instead, attention has focussed on weaker definitions of stability which are more easily achieved and are still useful for practical computations. One is *algebraic stability* (RT92; KLS87; LS91) which allows a linear growth in the transient solution of the form

$$\|U^{(n)}\| \leq \gamma n \|U^{(0)}\|, \quad (46)$$

where  $\gamma$  is again a uniform constant. A sufficient condition for algebraic stability is that

$$\tau(kA) \subset S, \quad (47)$$

where the numerical range  $\tau(kA)$  is a subset of the complex domain defined by

$$\tau(kA) = \left\{ k \frac{W^*AW}{W^*W} : W \neq 0 \right\} \quad (48)$$

in which  $W$  can be any non-zero complex vector of the required dimension and  $W^*$  is its Hermitian, the complex conjugate transpose. By considering  $W$  to be an eigenvector of  $A$ , it can be seen that  $k\lambda \in \tau(kA)$  for each eigenvalue of  $A$  and so the requirement that  $\tau(kA) \subset S$  is a tighter restriction on the maximum allowable timestep than asymptotic stability.

In the Navier-Stokes application, the main part of the analysis lies in bounding the range of the matrix  $M^{-1/2}(C+D)M^{-1/2}$ . The details are presented in Reference (Gil95a). The approach is to determine a timestep  $k$  such that  $\tau(kM^{-1/2}(C+D)M^{-1/2}) \subset V \subset S$ , with the subset  $V$  being either a rectangle or a half-circle. This leads to a sufficient condition for stability for time-accurate computations. With appropriate modifications to the matrix  $M$ , a sufficient stability limit for local timesteps for steady-state computations is also derived.

#### 5.4. NUMERICAL EXPERIMENTS

Figure 7 shows two sets of numerical experiments used to verify the stability analysis and determine how close the predicted sufficient stability limit is to the actual stability limit. The numerical tests used a tetrahedral grid created from a  $10 \times 10 \times 10$  Cartesian grid by cutting each hexahedron into six tetrahedra. Periodic boundary conditions were applied on all sides. In each case, a set of calculations was performed for a range of values for the CFL parameter  $r$  in increments of 0.25 starting from  $r = 2.75$ .

In the inviscid test case the Mach number was 0.5, and there was a grid stretching ratio of 10:1 in one direction. The algebraic stability theory predicts stability for  $r < 2.828$ . The numerical results shows stability up to  $r \approx 3.4$  so the sufficient stability theory underpredicts the stability boundary by approximately 15%.

In the viscous test case, the grid stretching ratio was increased to 100:1, representative of a boundary layer grid. The cell Reynolds number was chosen to be 1.0, making the viscous and inviscid terms equally important. In this case the algebraic stability analysis predicts stability for  $r < 2.616$ . The actual stability boundary is at  $r \approx 3.9$  so the theory underpredicts the maximum stable timestep by approximately 33%.

#### 5.5. CONCLUSIONS

The numerical experiments verify the usefulness of this algebraic stability analysis. The sufficient stability limits given by the theory do indeed lead

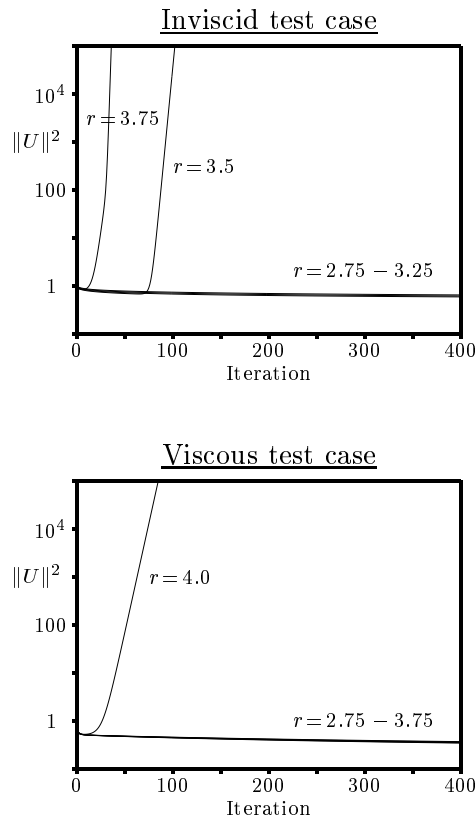


*Figure 7.* Numerical energy growth in two test cases

to stable computations, and they are not very much smaller than the actual stability limits determined experimentally. The ability to analyse the stability of complex systems of equations such as the discrete Navier-Stokes equations is very useful. The same method of analysis could also be used to examine the stability of different forms of upwinding on unstructured grids, or the stability of discrete boundary conditions on either structured or unstructured grids.

## 6. Final comments

The four analyses in this paper have illustrated the application of both well-established and very recent numerical analysis theory to problems of immediate relevance to practical CFD computations. Referring back to the list of challenges posed in the introduction, these analyses have dealt with systems of equations, nonlinearity (1), boundary conditions and multidisciplinary applications (2, 3), and high Reynolds number viscous flow and unstructured grids (4).

As CFD researchers tackle increasingly difficult applications in the future, it is my belief that, more and more, algorithm development will have to be based on a firm foundation of numerical analysis of this kind, analysing model problems which retain much of the complexity of the real computations.

## Acknowledgements

I wish to thank Rolls-Royce plc, EPSRC and DTI for funding the research reported in this paper.

## References

- S. Abarbanel and D. Gottlieb. Optimal time splitting for two- and three-dimensional Navier-Stokes equations with mixed derivatives. *Journal of Computational Physics*, 35:1–33, 1981.
- R.S. Amano, K.D. Wang, and V. Pavelic. A study of rotor cavities and heat transfer in a cooling process in a gas turbine. *J. Turbomachinery*, 116:333–338, 1994.
- D. Bohn, G. Lang, H. Schönenborn, and B. Bonhoff. Determination of thermal stress and strain based on a combined aerodynamic and thermal analysis for a turbine nozzle guide vane. ASME Paper 95-CTP-89, 1995.
- P. Crumpton and M.B. Giles. Aircraft computations using multigrid and an unstructured parallel library. AIAA Paper 95-0210, 1995.
- J. Chew, I.J. Taylor, and J.J. Bonsell. CFD developments for turbine blade heat transfer. In *3rd International Conference on Reciprocating Engines and Gas Turbines, I. Mech E., London*, C499-035, 1994.
- J.F. Dannenhoffer, III. A comparison of two adaptive grid techniques. In *Numerical Grid Generation in Computational Fluid Mechanics*. Pineridge Press Ltd, 1988.
- M.B. Giles. Energy stability analysis of multi-step methods on unstructured meshes. Technical Report CFDL-87-1, MIT Dept. of Aero. and Astro., 1987.
- M.B. Giles. Stability analysis of Galerkin/Runge–Kutta Navier–Stokes discretisations on unstructured grids. AIAA Paper 95-1753, 1995.
- M.B. Giles. Stability analysis of numerical interface boundary conditions for parabolic equations. Technical Report NA95/12, Oxford University Computing Laboratory, Wolfson Building, Parks Road, Oxford, OX1 3QD., 1995.
- M.B. Giles. Stability and accuracy of numerical boundary conditions in aeroelastic analysis. Technical Report NA95/13, Oxford University Computing Laboratory, Wolfson Building, Parks Road, Oxford, OX1 3QD., 1995.
- M.B. Giles. Analysis of the accuracy of shock-capturing in the steady quasi-1D Euler equations. *CFD Journal*, 5(2):99–108, 1996.

- S.K. Godunov and V.S. Ryabenkii. *The Theory of Difference Schemes—An Introduction*. North Holland, Amsterdam, 1964.
- B. Gustafsson and A. Sundström. Incompletely parabolic problems in fluid dynamics. *SIAM J. Appl. Math.*, 35(2):343–357, 1978.
- G.P. Guruswamy. ENSAERO — a multidisciplinary program for fluid/structural interaction studies of aerospace vehicles. *Comput Systems Engrg*, 1(2–4):237–256, 1990.
- G.P. Guruswamy. Unsteady aerodynamic and aeroelastic calculations for wings using Euler equations. *AIAA J.*, 28(3), 1990.
- A. Heselhaus and D.T. Vogel. Numerical simulation of turbine blade cooling with respect to blade heat conduction and inlet temperature profiles. AIAA Paper 95-3041, 1995.
- A. Jameson. Time dependent calculations using multigrid with applications to unsteady flows past airfoils, wings and rotors. AIAA Paper 91-1596, 1991.
- J.F.B.M. Kraaijevanger, H.W.J. Lenferink, and M.N. Spijker. Stepsize restrictions for stability in the numerical solution of ordinary and partial differential equations. *J. Comput. Appl. Math.*, 20:67–81, Nov 1987.
- H.O. Kreiss and L. Wu. On the stability definition of difference approximations for the initial boundary value problem. *Appl. Num. Math.*, 12:213–227, 1993.
- R. Löhner, K. Morgan, and O. Zienkiewicz. *Adaptive grid refinement for the compressible Euler equations*, pages 281–297. John Wiley and Sons Ltd, 1986.
- C. Lubich and O. Nevanlinna. On resolvent conditions and stability estimates. *BIT*, 31:293–313, 1991.
- H.W.J. Lenferink and M.N. Spijker. On the use of stability regions in the numerical analysis of initial value problems. *Math. Comp.*, 57(195):221–237, 1991.
- J.G. Marshall and M. Imregun. A 3D time-domain flutter prediction method for turbomachinery blades. In *Proc. Int. Forum on Aeroelasticity and Structural Dynamics, Royal Aeronautical Society, Manchester*, 1995.
- D. Mavriplis and A. Jameson. Multigrid solution of the Euler equations on unstructured and adaptive meshes. In S. McCormick, editor, *Proceedings of the Third Copper Mountain Conference on Multigrid Methods: Lecture Notes in Pure and Applied Mathematics*. Marcel Dekker Inc, 1987.
- J. Moore, J. G. Moore, G. S. Henry, and U. Chaudry. Flow and heat transfer in turbine tip gaps. *Journal of Turbomachinery*, 111:301–309, July 1989.
- T. Nomura and T.J.R. Hughes. An arbitrary Lagrangian–Eulerian finite element method for interaction of fluid and a rigid body. *Comput. Methods Appl. Mech. Engrg.*, 95:115–138, 1992.
- J. Peraire, J. Peiró, and K. Morgan. Finite element multigrid solution of Euler flows past installed aero-engines. *Comput. Mech.*, 11:433–451, 1993.
- J. Peraire, M. Vahdati, K. Morgan, and O.C. Zienkiewicz. Adaptive remeshing for compressible flow computations. *J. Comput. Phys.*, 72:449–466, 1987.
- R.D. Rausch, J.T. Batina, and H.T.Y. Yang. Three-dimensional time-marching aeroelastic analyses using an unstructured-grid Euler method. *AIAA J.*, 31(9):1626–1633, 1993.
- S.C. Reddy. *Pseudospectra of Operators and Discretization Matrices and an Application to Stability of the Method of Lines*. PhD thesis, Massachusetts Institute of Technology, Cambridge, Massachusetts 02139, 1991. Numerical Analysis Report 91-4.
- R.D. Richtmyer and K.W. Morton. *Difference Methods for Initial-Value Problems*. Wiley-Interscience, 2nd edition, 1967. Reprint edn (1994) Krieger Publishing Company, Malabar.
- S.C. Reddy and L.N. Trefethen. Lax-stability of fully discrete spectral methods via stability regions and pseudo-eigenvalues. *Comput. Methods Appl. Mech. Engrg.*, 80:147–164, 1990.
- S.C. Reddy and L.N. Trefethen. Stability of the method of lines. *Numer. Math.*, 62:235–267, 1992.
- J.L.M. van Dorselaer and J.F.B. Kraaijevanger. Linear stability analysis in the numerical solution of initial value problems. *Acta Numer.*, pages 199–237, 1993.

N.P. Weatherill, O. Hassan, M.J. Marchant, and D.L. Marcum. Adaptive inviscid flow solutions for aerospace geometries on efficiently generated unstructured tetrahedral meshes. AIAA Paper 93-3390, 1993.